Hollow Metallic and Dielectric Waveguides for Long Distance Optical Transmission and Lasers

By E. A. J. MARCATILI and R. A. SCHMELTZER

(Manuscript received June 12, 1964)

The field configurations and propagation constants of the normal modes are determined for a hollow circular waveguide made of dielectric material or metal for application as an optical waveguide. The increase of attenuation due to curvature of the axis is also determined.

The attenuation of each mode is found to be proportional to the square of the free-space wavelength λ and inversely proportional to the cube of the cylinder radius a. For a hollow dielectric waveguide made of glass with $\nu = 1.50$, $\lambda = 1\mu$, and $a = 1$ mm, an attenuation of 1.85 db/km is predicted for the minimum-loss mode, EH_{11}. This loss is doubled for a radius of curvature of the guide axis $R \approx 10$ km. Hence, dielectric materials do not seem suitable for use in hollow circular waveguides for long distance optical transmission because of the high loss introduced by even mild curvature of the guide axis. Nevertheless, dielectric materials are shown to be very attractive as guiding media for gaseous amplifiers and oscillators, not only because of the low attenuation but also because the gain per unit length of a dielectric tube containing He-Ne "masing" mixture at the right pressure can be considerably enhanced by reducing the tube diameter. In this application, a small guide radius is desirable, thereby making the curvature of the guide axis not critical. For $\lambda = 0.6328\mu$ and optimum radius $a = 0.058$ mm, a maximum theoretical gain of 7.6 db/m is predicted.

It is shown that the hollow metallic *circular waveguide is far less sensitive to curvature of the guide axis. This is due to the comparatively large complex dielectric constant exhibited by metals at optical frequencies. For a wavelength $\lambda = 1\mu$ and a radius $a = 0.25$ mm, the attenuation for the minimum loss TE_{01} mode in an aluminum waveguide is only 1.8 db/km. This loss is doubled for a radius of curvature as short as $R \approx 48$ meters. For $\lambda = 3\mu$ and $a = 0.6$ mm, the attenuation of the TE_{01} mode is also 1.8 db/km. The radius of curvature which doubles this loss is approximately 75 meters. The*

straight guide loss for the EH_{11} mode for $\lambda = 1\mu$ and $a = 0.25$ mm is 57 db/km and is increased to 320 db/km for $\lambda = 3\mu$ and $a = 0.6$ mm.

In view of the low-loss characteristic of the TE_{01} mode in metallic waveguides, the high-loss discrimination of noncircular electric modes, and the relative insensitivity to axis curvature, the hollow metallic *circular waveguide appears to be very attractive as a transmission medium for long distance optical communication.*

I. INTRODUCTION

During recent years the potentially large frequency range made available to communications by the development of the optical maser has stimulated much interest in efficient methods for long distance transmission of light. The most promising contenders for long distance optical transmission media consist of sequences of lenses or mirrors, highly reflective hollow metallic pipes, and dielectric waveguides.[1-10]

In this paper we present an analysis of the field configurations and propagation constants of the normal modes in a hollow circular waveguide which, because of its simplicity and low loss, may become an important competitor. The guiding structure considered here may consist of an ordinary metallic pipe of precision bore whose inner surface is highly reflective, or of a hollow dielectric pipe — i.e., one in which the metal is replaced with dielectric. Although the transmission characteristics of metallic waveguides are well known for microwave frequencies, this theory is invalidated for operation at optical wavelengths, because the metal no longer acts as a good conductor but rather as a dielectric having a large dielectric constant. In the subsequent analysis, therefore, both the dielectric and metallic guide are considered as special cases of a general hollow circular waveguide having an external medium made of arbitrary isotropic material whose optical properties are characterized by a finite complex refractive index. If the free-space wavelength is much smaller than the internal radius of the tube, the energy propagates not in the external medium but essentially within the tube, bouncing at grazing angles against the wall. Consequently, there is little energy loss due to refraction. The refracted field is partially reflected by the external surface of the tube and may, in general, interfere constructively or destructively with the field inside the tube, decreasing or increasing the attenuation. Because of the difficulty of controlling the interference paths, it seems more convenient to eliminate the effect completely by introducing sufficient loss in the dielectric or, in the case of a glass dielectric, by frosting the external surface. The field in the hole of the

tube is then unaffected by wall thickness. We shall therefore simplify the analysis of the hollow circular waveguide by assuming infinite wall thickness, as depicted in Fig. 1.

This structure will be shown to be attractive as a low-loss transmission medium for long distance optical communication as well as for optical gaseous amplifiers and oscillators. It is known, for example, that in a tube containing a He-Ne mixture such that the product of radius and pressure is roughly a constant, the gain per unit length is inversely proportional to the radius of the tube.[11] On the other hand, we find in this paper that the attenuation of the normal modes is inversely proportional to the cube of the radius. Hence there is an optimum tube radius for which the net gain per unit length is a maximum. Furthermore, because the guidance is continuous, there is no need for periodic focusing. Consequently, no restriction need be imposed on the length of the amplifying or oscillating tube.

We begin by analyzing an idealized guide having a straight axis and a cylindrical wall. The results are then extended to include the effects of mild curvature of the guide axis by finding a perturbation correction for field configurations and propagation constants of the idealized straight guide.

II. MODAL ANALYSIS OF THE GENERAL STRAIGHT CIRCULAR WAVEGUIDE

Consider a waveguide consisting of a circular cylinder of radius a and free-space dielectric constant ϵ_0 embedded in another medium of dielectric or metal having a complex dielectric constant ϵ. The magnetic permeability μ_0 is assumed to be that of free space for both media. We are interested in finding the field components of the normal modes of the waveguide and in determining the complex propagation constants of these modes.

The problem is substantially simplified if it is assumed that

$$ka = 2\pi a/\lambda \gg |\nu| u_{nm} \tag{1}$$

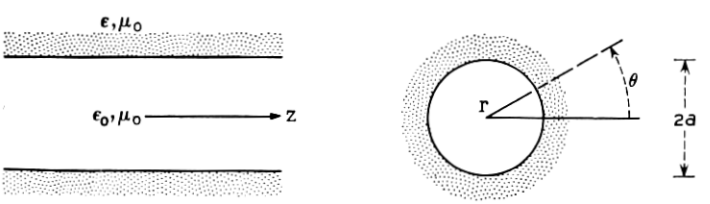

Fig. 1 — Hollow dielectric waveguide.

and

$$| (\gamma/k) - 1 | \ll 1 \tag{1}$$

where $k = \omega\sqrt{\epsilon_0\mu_0} = 2\pi/\lambda$ is the free-space propagation constant; u_{nm} is the mth root of the equation $J_{n-1}(u_{nm}) = 0$, and n and m are integers that characterize the propagating mode; $\nu = \sqrt{\epsilon/\epsilon_0}$ is the complex refractive index of the external medium; and γ is the axial propagation constant of the mode under consideration. The first inequality states that the radius a is much larger than the free-space wavelength λ. In the case of metalization of the external medium, $| \nu |$ may be quite large but is finite at optical frequencies. The second inequality restricts our analysis to low-loss modes, which are those whose propagation constants γ are nearly equal to that of free space.

The field components of the natural modes of the most general circular cylindrical structure with arbitrary isotropic internal and external media have been determined by Stratton.[12] This structure supports three types of modes: first, transverse circular electric modes whose only field components are E_θ, H_r and H_z; second, transverse circular magnetic modes whose components are H_θ, E_r and E_z; and third, hybrid modes with all the electric and magnetic components present. The approximate field components of these modes are written below. They have been derived using the inequalities (1) and neglecting terms with powers of λ/a larger than one. The superscripts i and e refer to the internal and external media, respectively.

1. Circular electric modes TE_{0m} $(n = 0)$

$$\left.\begin{aligned} E_{\theta 0m}{}^{i} &= J_1(k_i r) \\ H_{r0m}{}^{i} &= -\sqrt{\frac{\epsilon_0}{\mu_0}}\, J_1(k_i r) \\ H_{z0m}{}^{i} &= -i\sqrt{\frac{\epsilon_0}{\mu_0}}\,\frac{u_{0m}}{ka}\, J_0(k_i r) \end{aligned}\right\} \exp i(\gamma z - \omega t)$$

$$\left.\begin{aligned} E_{\theta 0m}{}^{e} &= -1 \\ H_{r0m}{}^{e} &= \sqrt{\frac{\epsilon_0}{\mu_0}} \\ H_{z0m}{}^{e} &= -i\sqrt{\nu^2 - 1}\,\sqrt{\frac{\epsilon_0}{\mu_0}} \end{aligned}\right\} i\,\frac{u_{0m}}{k\sqrt{ar(\nu^2 - 1)}}\, J_0(u_{0m}) \exp i[k_e(r - a) + \gamma z - \omega t] \tag{2}$$

2. Circular magnetic modes TM_{0m} $(n = 0)$

$$\left.\begin{aligned}
&\left.\begin{aligned}
E_{r0m}{}^{i} &= J_1(k_i r)\\
E_{z0m}{}^{i} &= i\,\frac{u_{0m}}{ka}\,J_0(k_i r)\\
H_{\theta 0m}{}^{i} &= \sqrt{\frac{\epsilon_0}{\mu_0}}\,J_1(k_i r)
\end{aligned}\right\}\ \exp i(\gamma z - \omega t)\\
&\left.\begin{aligned}
E_{r0m}{}^{e} &= -\frac{1}{\nu^2}\\
E_{z0m}{}^{e} &= \sqrt{\nu^2 - 1}\\
H_{\theta 0m}{}^{e} &= -\sqrt{\frac{\epsilon_0}{\mu_0}}
\end{aligned}\right\}\ i\,\frac{u_{0m}J_0(u_{0m})}{k\sqrt{ar(\nu^2 - 1)}}\exp i\,[k_e(r-a) + \gamma z - \omega t]
\end{aligned}\right\}. \qquad (3)$$

3. Hybrid modes EH_{nm} $(n \neq 0)$

$$\left.\begin{aligned}
&\left.\begin{aligned}
E_{\theta nm}{}^{i} &= \left[J_{n-1}(k_i r) + \frac{iu_{nm}{}^2}{2nka}\sqrt{\nu^2 - 1}\,J'_n(k_i r)\right]\\
&\qquad\qquad \cdot\cos n(\theta + \theta_0)\\
E_{rnm}{}^{i} &= \left[J_{n-1}(k_i r) + \frac{iu_{nm}}{2kr}\sqrt{\nu^2 - 1}\,J_n(k_i r)\right]\\
&\qquad\qquad \cdot\sin n(\theta + \theta_0)\\
E_{znm}{}^{i} &= -i\,\frac{u_{nm}}{ka}\,J_n(k_i r)\,\sin n(\theta + \theta_0)
\end{aligned}\right\}\ \exp i(\gamma z - \omega t)\\
&H_{\theta nm}{}^{i} = \sqrt{\frac{\epsilon_0}{\mu_0}}\,E_{rnm}{}^{i}\\
&H_{rnm}{}^{i} = -\sqrt{\frac{\epsilon_0}{\mu_0}}\,E_{\theta nm}{}^{i}\\
&H_{znm}{}^{i} = -\sqrt{\frac{\epsilon_0}{\mu_0}}\,E_{znm}{}^{i}\,\mathrm{ctn}\,n(\theta + \theta_0)\\
&\left.\begin{aligned}
E_{\theta nm}{}^{e} &= \cos n(\theta + \theta_0)\\
E_{rnm}{}^{e} &= \sin n(\theta + \theta_0)\\
E_{znm}{}^{e} &= -\sqrt{\nu^2 - 1}\,\sin n(\theta + \theta_0)
\end{aligned}\right\}\ i\,\frac{u_{nm}}{k\sqrt{ar(\nu^2 - 1)}}\,J_n(u_{nm})\\
&\qquad\qquad \cdot\exp i[k_e(r - a) + \gamma z - \omega t]\\
&H_{\theta nm}{}^{e} = \nu^2\sqrt{\frac{\epsilon_0}{\mu_0}}\,E_{rnm}{}^{e}\\
&H_{rnm}{}^{e} = -\sqrt{\frac{\epsilon_0}{\mu_0}}\,E_{\theta nm}{}^{e}\\
&H_{znm}{}^{e} = -\sqrt{\frac{\epsilon_0}{\mu_0}}\,E_{znm}{}^{e}\,\mathrm{ctn}\,n(\theta + \theta_0)
\end{aligned}\right\} \qquad (4)$$

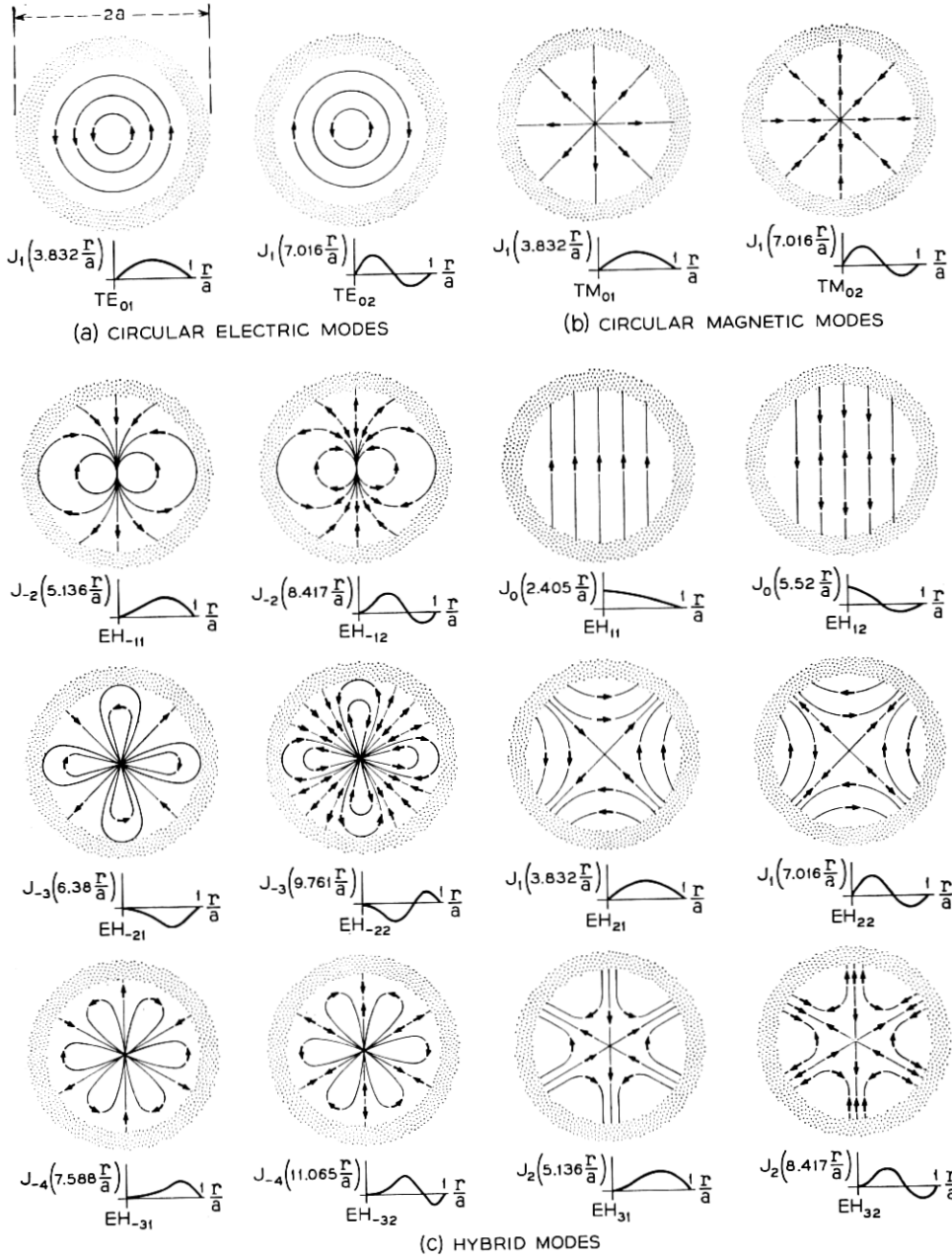

Fig. 2 — Electric field lines of modes in hollow dielectric waveguides: (a) circular electric modes, (b) circular magnetic modes, (c) hybrid modes.

where the complex propagation constant γ satisfies the relationships

$$\begin{aligned} k_i^2 &= k^2 - \gamma^2 \\ k_e^2 &= \nu^2 k^2 - \gamma^2 \end{aligned} \tag{5}$$

and u_{nm} is the mth root of the equation

$$J_{n-1}(u_{nm}) = 0. \tag{6}$$

As usual, $| n |$ is the number of periods of each field component in the θ direction, and m is both the order of the root of (6) and the number of maxima and minima of each component counted in the radial direction within the internal medium. The constant θ_0 appearing in (4) will become of interest later on when we study the waveguide with curved axis, because it will admit any orientation of the transverse electric field relative to the plane of curvature of the guide axis.

For $n = 0$, the modes are either transverse electric TE_{0m} (2), or transverse magnetic TM_{0m} (3). The lines of electric field of the TE_{0m} modes are transverse concentric circles centered on the z axis. The lines of magnetic field are in planes containing the z axis. Similarly, the lines of magnetic field of the TM_{0m} modes are transverse concentric circles centered on the z axis with the electric field contained in radial planes. The electric field lines of the modes TE_{01}, TE_{02}, TM_{01} and TM_{02} are shown in Figs. 2(a) and 2(b); each vector represents qualitatively the intensity and direction of the local field.

For $n \neq 0$, the modes are hybrid, EH_{nm} (4); therefore, the magnetic and electric field are three-dimensional with relatively small axial field components in the internal medium. Thus the hybrid modes are almost transverse.

Let us examine the projection of these three-dimensional field lines on planes perpendicular to the axis z of the waveguide. The differential equations for the projected lines of electric field in both media are

$$\begin{aligned} \frac{1}{r}\frac{dr}{d\theta} &= \frac{E_{rnm}{}^i}{E_{\theta nm}{}^i} \\ \frac{1}{r}\frac{dr}{d\theta} &= \frac{E_{rnm}{}^e}{E_{\theta nm}{}^e}. \end{aligned} \tag{7}$$

$E_{rnm}{}^i$ as well as $E_{\theta nm}{}^i$ contain two terms as given in (4). Both are necessary to satisfy the boundary conditions. If we neglect the second term, however, no substantial error is introduced except very close (a few wavelengths) to the boundary, where the second term dominates as

the first tends to zero. With this simplification, the differential equations (7) in both media become identical

$$(1/r)(dr/d\theta) = \tan n\theta.$$

Upon integrating, one obtains an equation for the locus of the projected electric field lines

$$(r/r_0)^n \cos n\theta = 1 \tag{8}$$

where r_0 is a constant of integration that individualizes the member of the family of lines. The electric field of an EH_{nm} mode is different from that of EH_{-nm} mode.

The projection of the magnetic field lines is determined in a similar way. These equations are

$$(r/r_0)^n \sin n\theta = 1 \tag{9}$$

for the internal medium and

$$(r/r_0)^{n\nu^2} \sin n\theta = 1$$

for the external medium.

The projections of the internal electric (8) and magnetic (9) field lines are identical for any given mode except for a rotation of $\pi/(2n)$ radians around the z axis. In Fig. 2(c) the lines of the electric field in the internal medium are depicted for the first few hybrid modes. Again the vectors represent qualitatively the field intensities and directions.

What happens at the boundary? Consider, for example, the projected electric lines of mode EH_{11}, as shown in Fig. 3(a). These field lines satisfy (8), an equation which is valid everywhere except near the boundary. The boundary conditions are violated in Fig. 3(a) because there is continuity not only of the tangential electric component but also of the normal component. The internal normal component must be ν^2 times larger than the external one. Consequently, the electric field line must be discontinuous. This result is shown qualitatively in Fig. 3(b).

A three-dimensional representation of the field lines is far more complicated than the two-dimensional one depicted in Fig. 2. As a typical example, the electric field lines of the EH_{22} mode are shown in Fig. 4 in a three-dimensional perspective.

The propagation constants of the TE_{0m}, TM_{0m} and EH_{nm} ($n \neq 0$) modes are determined below (21). It is found that the hybrid mode $EH_{-|n|,m}$ is degenerate (same propagation constant) with the $EH_{|n|+2,m}$; i.e., for every hybrid mode with negative azimuthal index there is a degenerate hybrid mode with positive aximuthal index. The

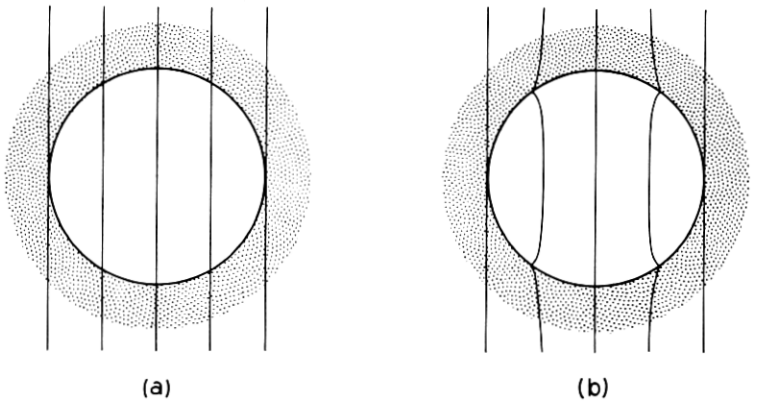

Fig. 3 — (a) Electric field lines of EH_{11} mode violating boundary conditions; (b) same EH_{11} mode with electric field lines qualitatively corrected.

transverse modes TE_{0m} and TM_{0m} and the hybrid modes EH_{1m} and EH_{2m} have no degenerate counterpart.

If the field components of the degenerate $EH_{-|n|,m}$ and $EH_{|n|+2,m}$ modes (4) are added, we obtain new composite modes whose electric and magnetic field lines project as straight lines on a plane perpendicular to the z axis. Some of those composite modes are shown in Fig. 5.

It should be noted that if the refractive index of the external medium,

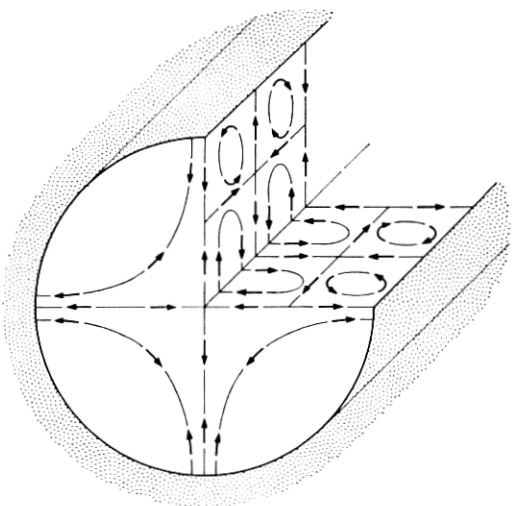

Fig. 4 — Cutaway view of electric field lines of EH_{22} mode. The axial period is grossly exaggerated.

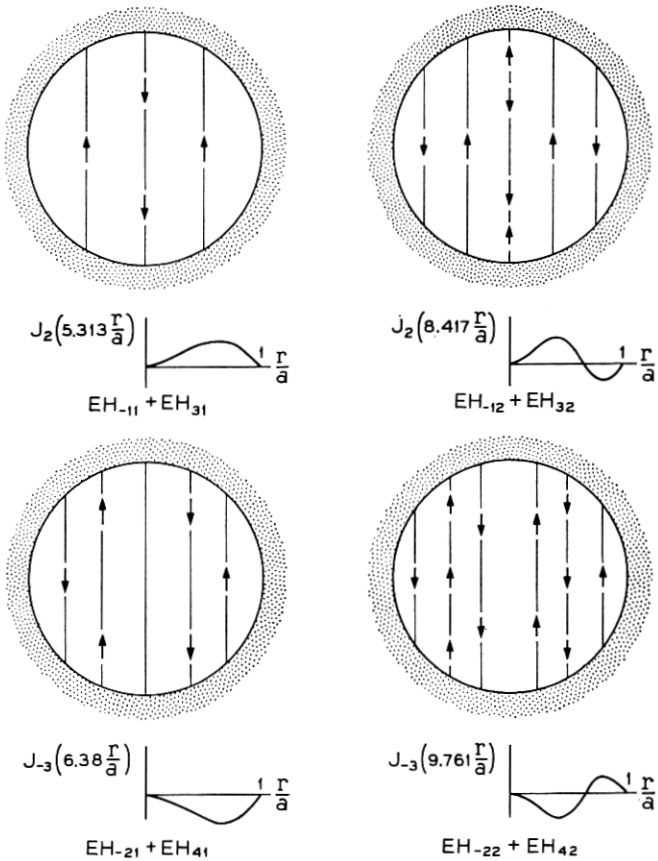

Fig. 5 — Electric field lines of composite modes $EH_{-|n|,m} + EH_{|n|+2,m}$.

ν, is very close to unity, then for each value of m, the TE_{0m}, TM_{0m} and EH_{2m} modes also become degenerate (17), (21) and the sum of the components of TE_{0m} (2) and EH_{2m} (4) yields a new composite mode, as shown in Fig. 6. This mode, together with those in Fig. 5 and the EH_{1m} of Fig. 2(c), form a complete set that closely resembles the set found for interferometers with plane circular mirrors or for sequences of circular irises.[1]

Let us now consider the field intensity distribution outside and inside the hollow dielectric waveguide. The external field (2), (3) and (4) has the radial dependence

$$\frac{\exp\left[ik_e(r-a)\right]}{\sqrt{r}}.$$

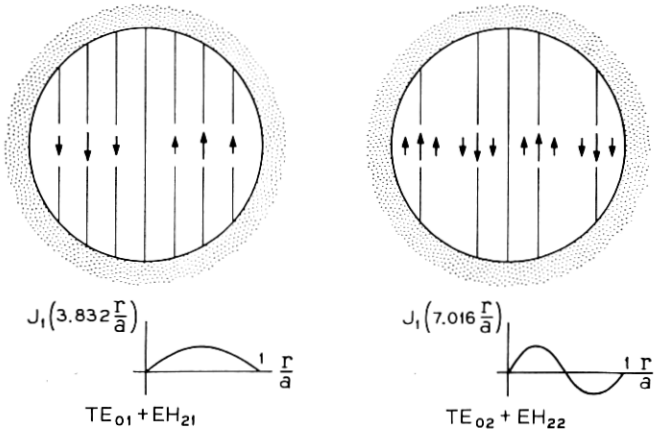

Fig. 6 — Electric field lines of composite modes $TE_{0m} + EH_{2m}$.

From (5) and (20) we obtain, neglecting terms of order $(\lambda/a)^2$ and higher, $k_e = k\sqrt{\nu^2 - 1}$. The radial dependence is then

$$\frac{\exp\left[ik\sqrt{\nu^2 - 1}(r - a)\right]}{\sqrt{r}}.$$

If the dielectric is lossy, the refractive index ν has a positive imaginary part. The external electric and magnetic fields then oscillate with period of the order of $\lambda/|\sqrt{\nu^2 - 1}|$ and decay exponentially in the radial direction. The maximum field intensities in the external medium occur at the boundary $r = a$. Being proportional to λ/a, these maxima are small.

The field intensity inside the hollow waveguide is more interesting. Again if we substitute γ (20) into (2), (3) and (4) and neglect terms of the order λ/a, only the internal transverse components remain.

For TE_{0m} modes

$$E_{\theta 0m}{}^i = -\sqrt{\frac{\mu_0}{\epsilon_0}}\, H_{r0m}{}^i = J_1\left(u_{0m}\frac{r}{a}\right). \tag{10}$$

For TM_{0m} modes,

$$E_{r0m}{}^i = \sqrt{\frac{\mu_0}{\epsilon_0}}\, H_{\theta 0m}{}^i = J_1\left(u_{0m}\frac{r}{a}\right). \tag{11}$$

For EH_{nm} modes,

$$E_{\theta nm}{}^{i} = -\sqrt{\frac{\mu_0}{\epsilon_0}}\, H_{rnm}{}^{i} = J_{n-1}\left(u_{nm}\frac{r}{a}\right)\cos n\theta$$
$$E_{rnm}{}^{i} = \sqrt{\frac{\mu_0}{\epsilon_0}}\, H_{\theta nm}{}^{i} = J_{n-1}\left(u_{nm}\frac{r}{a}\right)\sin n\theta. \tag{12}$$

The field components of each mode have approximately the same radial dependence, varying as Bessel functions of the first kind, and tending to negligibly small values at the boundary (6). This approximate radial dependence (10), (11) and (12) is reproduced under each mode pattern in Figs. 2(a), 2(b) and 2(c).

III. PROPAGATION CONSTANTS FOR THE GENERAL CIRCULAR CYLINDRICAL GUIDE

In this section we shall determine the propagation constants γ, of the TE_{0m}, TM_{0m} and EH_{nm} modes in the straight hollow guide at optical wavelengths. The propagation constants are the roots of the following characteristic equation for the general circular cylindrical structure.[12] They are related to k_i and k_e by expressions (5).

$$\left[\frac{J_n'(k_ia)}{J_n(k_ia)} - \frac{k_i}{k_e}\frac{H_n^{(1)'}(k_ea)}{H_n^{(1)}(k_ea)}\right]\left[\frac{J_n'(k_ia)}{J_n(k_ia)} - \frac{\nu^2 k_i}{k_e}\frac{H_n^{(1)'}(k_ea)}{H_n^{(1)}(k_ea)}\right] = \left[\frac{n\lambda}{kk_ia}\right]^2\left[1 - \left(\frac{k_i}{k_e}\right)\right]^2. \tag{13}$$

This equation is simplified substantially when the approximations in (1) are introduced. Since $k_ea \gg 1$, the asymptotic value of the Hankel functions may be used

$$\frac{H_n^{(1)'}(k_ea)}{H_n^{(1)}(k_ea)} \approx i + 0(1/k_ea), \qquad k_ea \gg 1. \tag{14}$$

Since

$$\frac{\nu^2}{k_ea} \approx \frac{\nu^2}{(\nu^2-1)^{\frac{1}{2}}}\left(\frac{\lambda}{2\pi a}\right) \ll 1 \tag{15}$$

powers of ν^2/k_ea larger than one shall be neglected. The characteristic equation then simplifies to

$$J_{n-1}(k_ia) = i\nu_n(k_i/k)J_n(k_ia) \tag{16}$$

where

$$\nu_n = \begin{cases} \dfrac{1}{\sqrt{\nu^2 - 1}} & \text{for } TE_{0m} \text{ modes } (n = 0) \\ \dfrac{\nu^2}{\sqrt{\nu^2 - 1}} & \text{for } TM_{0m} \text{ modes } (n = 0) \\ \dfrac{\frac{1}{2}(\nu^2 + 1)}{\sqrt{\nu^2 - 1}} & \text{for } EH_{nm} \text{ modes } (n \neq 0). \end{cases} \tag{17}$$

To solve the characteristic equation for $k_i a$ we notice that because of (1) and (5), the right-hand side of (16) is close to zero. Using a perturbation technique and keeping only the first term of the perturbation,

$$k_i a \approx u_{nm}(1 - i\nu_n/ka) \tag{18}$$

where u_{nm} as before is the mth root of the equation

$$J_{n-1}(u_{nm}) = 0. \tag{19}$$

The validity of (18) is assured provided that the order of the mode is low enough so that $| \nu_n | u_{nm} \ll ka$. The propagation constants γ can then be obtained from (5)

$$\gamma \approx k\left[1 - \frac{1}{2}\left(\frac{u_{nm}\lambda}{2\pi a}\right)^2\left(1 - \frac{i\nu_n\lambda}{\pi a}\right)\right]. \tag{20}$$

The phase constant and attenuation constant of each mode are the real and imaginary parts of γ, respectively,

$$\begin{aligned} \beta_{nm} &= \text{Re } (\gamma) = \frac{2\pi}{\lambda}\left\{1 - \frac{1}{2}\left[\frac{u_{nm}\lambda}{2\pi a}\right]^2\left[1 + \text{Im}\left(\frac{\nu_n\lambda}{\pi a}\right)\right]\right\} \\ \alpha_{nm} &= \text{Im } (\gamma) = \left(\frac{u_{nm}}{2\pi}\right)^2 \frac{\lambda^2}{a^3} \text{Re } (\nu_n). \end{aligned} \tag{21}$$

IV. PROPAGATION CONSTANTS FOR STRAIGHT DIELECTRIC GUIDES

For guides made of dielectric material, ν_n is usually real and independent of λ, so that the phase and attenuation constants are

$$\left.\begin{aligned} \beta_{nm} &= \frac{2\pi}{\lambda}\left\{1 - \frac{1}{2}\left(\frac{u_{nm}\lambda}{2\pi a}\right)^2\right\} \\ \alpha_{nm} &= \left(\frac{u_{nm}}{2\pi}\right)^2 \frac{\lambda^2}{a^3} \begin{cases} \dfrac{1}{\sqrt{\nu^2 - 1}}, & \text{for } TE_{0m} \text{ modes } (n = 0) \\ \dfrac{\nu^2}{\sqrt{\nu^2 - 1}}, & \text{for } TM_{0m} \text{ modes } (n = 0) \\ \dfrac{\frac{1}{2}(\nu^2 + 1)}{\sqrt{\nu^2 - 1}}, & \text{for } EH_{nm} \text{ modes } (n \neq 0) \end{cases} \end{aligned}\right\}. \quad (22)$$

The phase constant of modes in hollow dielectric waveguides have the same frequency dependence as modes in perfectly conducting metallic waveguides when operating far from cutoff; both transmission media are then similarly dispersive.

The attenuation constants are proportional to λ^2/a^3. Consequently, the losses can be made arbitrarily small by choosing the radius of the tube a sufficiently large relative to the wavelength λ.

The refractive index ν affects the attenuation of each of the three types of modes (22) in different ways. This fact is reasonable on physical grounds. TE_{0m} modes can be considered to be composed of plane wavelets, each impinging at grazing angle on the interface between the two media with polarization perpendicular to the plane of incidence. It is known from the laws of refraction that the larger the value of ν, the smaller the refracted power.

TM_{0m} modes may also be thought of as consisting of plane wavelets, but with the electric field of each now contained in the plane of incidence. For ν very close to unity, there is little reflection and the refracted loss is high; as the value of ν is allowed to become large, each wavelet gets close to the Brewster angle of incidence and again the refracted loss is high. The minimum occurs for $\nu = \sqrt{2}$.

EH_{nm} modes are composed of both types of plane wavelets. Therefore, as is reasonable from the above argument, the attenuation constant α_{nm} has a ν dependence which is an average of those of TE_{0m} and TM_{0m} modes. The value of ν that minimizes α_{nm} is $\nu = \sqrt{3} = 1.73$.

The attenuation constants (22) are proportional to u_{nm}^2. Some values of u_{nm} (19) are presented in Table I. For a fixed value of n the attenuation constant increases with m. This statement is not true for m fixed and n variable.

Comparing the attenuation constants (22) of the different modes, we find that the mode with lowest attenuation is TE_{01} if $\nu > 2.02$ and EH_{11} if $\nu < 2.02$. Most glasses have a refractive index $\nu \approx 1.5$, and

TABLE I— SOME VALUES OF u_{nm}

n/m	1	2	3	4
1	2.405	5.52	8.654	11.796
2 or 0	3.832	7.016	10.173	13.324
3 or −1	5.136	8.417	11.62	14.796
4 or −2	6.380	9.761	13.015	16.223

consequently for hollow glass tube EH_{11} should be preferred. The attenuation of this mode ($8686\alpha_{11}$ in db/km) has been plotted in Fig. 7 as a function of λ/a for $\nu = 1.50$ using λ as a parameter. Typically, for a wavelength $\lambda = 1\mu$ and radius $a = 1$ mm, the attenuation of the EH_{11} mode is 1.85 db/km (≈3 db/mile). If the radius of the guide is doubled, the attenuation is reduced to 0.231 db/km.

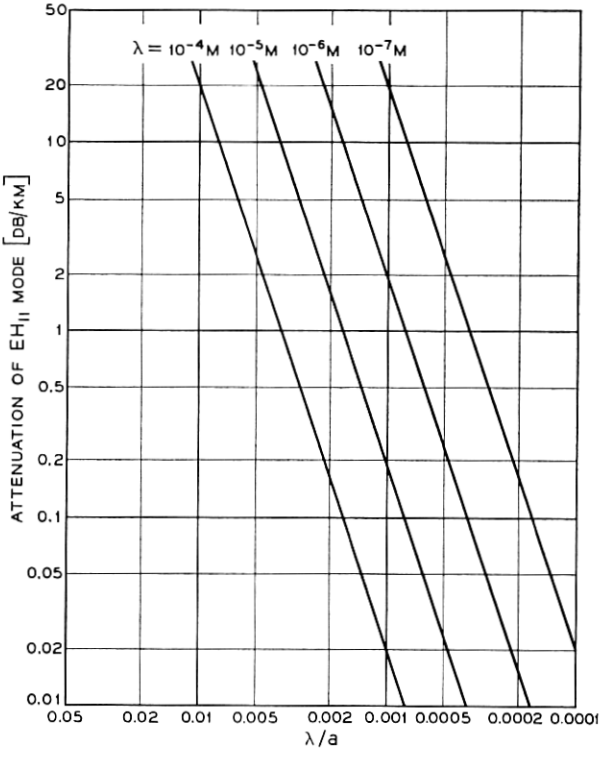

Fig. 7 — Attenuation of EH_{11} modes ($1.85\ \lambda^2/a^3$) versus wavelength/radius ($\nu = 1.5$).

V. HOLLOW DIELECTRIC WAVEGUIDE FOR OPTICAL MASER AMPLIFIERS AND OSCILLATORS

A mode traveling in a hollow dielectric waveguide filled with "masing" material experiences a net gain which is given by the difference between the amplification due to the active medium and the loss due to leakage through the walls. It has been shown[11] that in a tube filled with the right mixture of He and Ne at the proper pressure, the gain G is inversely proportional to the radius a of the tube. Then

$$G = (A/a) \text{ db/m} \tag{23}$$

where the radius a is measured in meters and the constant A is

$$A = 0.00066 \text{ db.}$$

On the other hand, we have found that the transmission loss of the EH_{11} mode in the hollow waveguide with a refractive index $\nu = 1.50$ is $L = 8.686\alpha_{11}$. From (22)

$$L = B(\lambda^2/a^3) \text{ db/m} \tag{24}$$

where the constant B is

$$B = 1.85 \text{ db.}$$

The net gain per unit length is then

$$G - L = (A/a) - B(\lambda^2/a^3) \tag{25}$$

passing through a maximum at the value of the radius for which

$$\partial(G - L)/\partial a = 0.$$

The optimum radius and the maximum net gain are respectively

$$\begin{aligned} a_{\text{opt}} &= \sqrt{3\frac{B}{A}}\,\lambda = 91.7\lambda \\ (G - L)_{\max} &= \frac{2}{3^{\frac{3}{2}}}\frac{A^{\frac{3}{2}}}{B^{\frac{1}{2}}}\frac{1}{\lambda} = 4.81\,\frac{10^{-6}}{\lambda} \text{ db/m.} \end{aligned} \tag{26}$$

For the He-Ne mixture, $\lambda = 0.6328\ 10^{-6}$ m. Consequently

$$\begin{aligned} a_{\text{opt}} &= 0.058 \text{ mm} \\ (G - L)_{\max} &= 7.6 \text{ db/m.} \end{aligned} \tag{27}$$

Although the diameter of the tube is quite small, the gain per unit length is sufficiently large as to make hollow dielectric amplifiers and oscillators attractive for experimentation.

Present-day confocal He-Ne masers employ tubes whose approximate length and radius are 1 m and 3 mm respectively. The gain per passage (23) is 0.22 db ($\approx$5 per cent). If a hollow dielectric waveguide with an optimum radius 0.058 mm were used, the same gain would be achieved with a length of only 0.22/7.6 = 29 mm. This presents an excellent possibility for a very compact maser.

Even for radii larger than the optimum, the hollow dielectric waveguide is still attractive. For example with $a = 0.25$ mm, the gain is 2.6 db/m, a value far larger than the gain 0.22 db/m obtained for the 3-mm radius tube commonly used for masers.

Nevertheless, for long-wavelength masers the optimum values (26) are not practical. Consider for example a tube containing an active material which amplifies at $\lambda = 10^{-4}$ m. Let us assume that the constant A is still 0.00066. Then from (26), the optimum radius and maximum gain are

$$\begin{aligned} a_{\text{opt}} &= 9.14 \text{ mm} \\ (G - L)_{\max} &= 0.0481 \text{ db/m}. \end{aligned} \tag{28}$$

The gain is very small. It could be enhanced by reducing the radius and by increasing the refractive index ν of the walls to a value much larger than 1.5. This can be accomplished if metal is used instead of dielectric, as is shown in the next section.

VI. ATTENUATION CONSTANTS FOR THE STRAIGHT METALLIC GUIDE

In order to discuss the attenuation characteristics of metallic waveguides, we shall need to have some quantitative information about the behavior of metals at optical frequencies. We examine as a typical example the optical properties of aluminum, even though this may not be the most suitable metal. The dispersion characteristics of the conductivity and relative dielectric constants of aluminum have been studied extensively by Hodgson,[13] Beattie and Conn,[14] and Schulz.[15] The data used below have been taken from a compilation of the results of these studies,[16] and is presented graphically in Fig. 8. It is evident from these dispersion curves that the dielectric constant for aluminum is much larger than for ordinary dielectrics and increases monotonically with wavelength in the range $0.3\mu < \lambda < 4.0\mu$.

The circular electric modes have the lowest loss in metallic waveguides, while the circular magnetic and hybrid modes are rapidly attenuated even for a wavelength as short as 0.3μ. The attenuation constant α_{01} for the lowest-loss TE_{01} mode is plotted in Fig. 9 for wave-

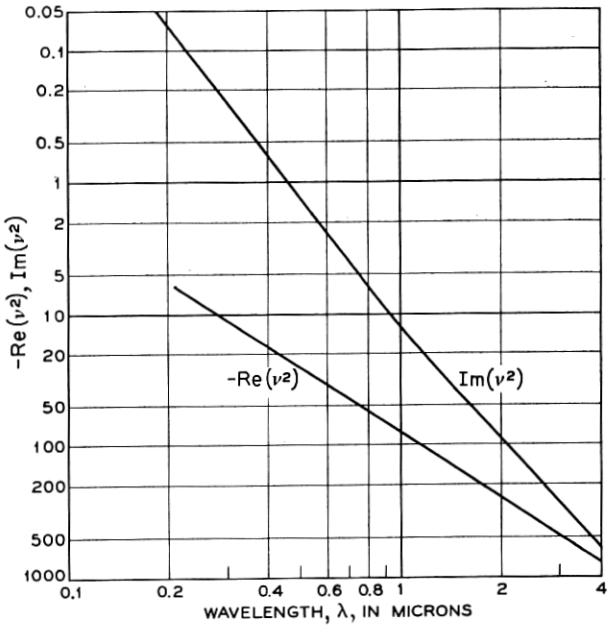

Fig. 8 — Dispersion curve for aluminum $\nu^2 = \epsilon/\epsilon_0 = \mathrm{Re}(\nu^2) + i\,\mathrm{Im}(\nu^2)$ versus wavelength $\lambda(\mu)$.

lengths in the range $0.3\mu < \lambda < 4.0\mu$ for $a = 0.25$ mm, 0.50 mm and 1 mm. These data show a considerable improvement over that corresponding to the lowest-loss mode EH_{11} for the dielectric guide. We saw that for a hollow glass dielectric waveguide, the EH_{11} mode has a loss of 1.8 db/km for a radius $a = 1$ mm and wavelength $\lambda = 1\mu$. The attenuation for the TE_{01} mode for the aluminum guide with the same radius and wavelength is only 0.028 db/km. For a wavelength $\lambda = 1\mu$ and a radius $a = 0.25$ mm, the minimum-loss TE_{01} mode for the aluminum waveguide has an attenuation constant $\alpha_{01} = 1.8$ db/km. The same attenuation is achieved for $\lambda = 3\mu$ and $a = 0.6$ mm. The attenuation constant for the TE_{02} mode under the last two conditions is $\alpha_{02} = 6.05$ db/km. For a wavelength $\lambda = 1\mu$ and $a = 0.25$ mm, the straight guide losses for the TM_{01} and EH_{11} modes are approximately 145 db/km and 57 db/km, respectively.

VII. FIELD CONFIGURATION AND ATTENUATION OF MODES IN THE CURVED GUIDE

In order to achieve a more realistic evaluation of the hollow circular waveguide for long distance optical transmission, it is necessary to

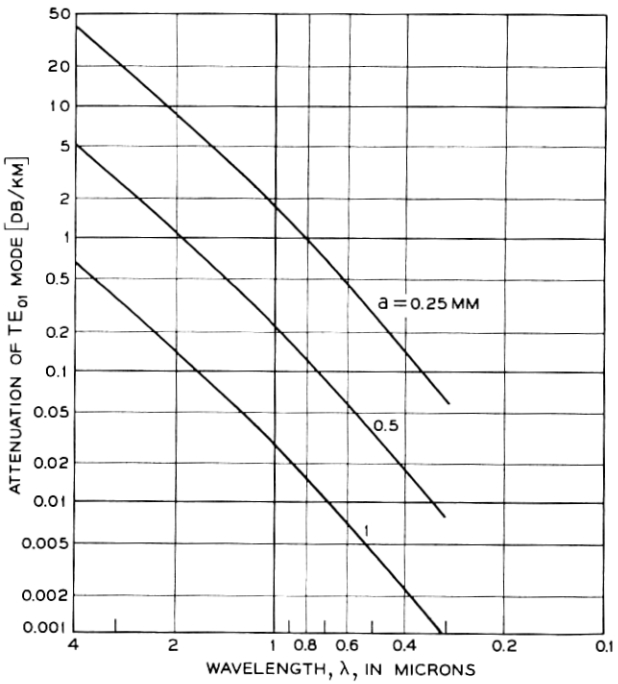

Fig. 9 — Attenuation of TE_{01} mode, α_{01} versus wavelength $\lambda(\mu)$, for aluminum guide.

evaluate the effects of mild curvature of the guide axis. This is most easily accomplished by determining a perturbation correction for both the field configuration and the attenuation constants for the idealized straight guide whose characteristics have been described above.

VIII. FORMULATION OF THE PROBLEM

Consider the toroidal system (r, θ, z) with metric coefficients

$$\begin{aligned} e_r &= 1 \\ e_\theta &= r \\ e_z &= 1 + r/R \sin \theta \end{aligned} \tag{29}$$

as depicted in Fig. 10. In this system of coordinates, a differential length is given by

$$ds = (e_r^2 dr^2 + e_\theta^2 d\theta^2 + e_z^2 dz^2)^{\frac{1}{2}} \tag{30}$$

where R is the radius of curvature of the toroidal system and is chosen

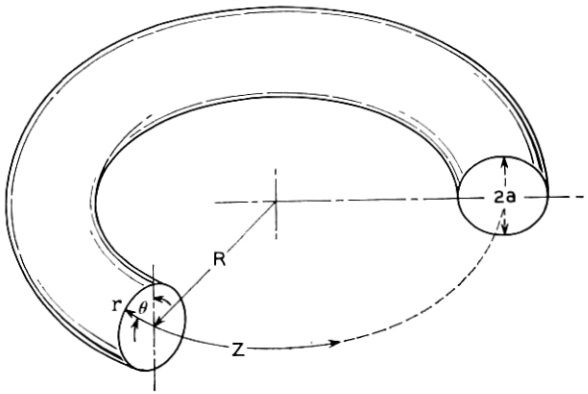

Fig. 10 — The curved hollow dielectric waveguide and the associated toroidal coordinate system (r, θ, Z).

equal to the radius of curvature of the guide axis, so that the guide wall is located at $r = a$, and the axis of the guide coincides with the curved z-axis. In this toroidal coordinate system, Maxwell's equations are

$$\begin{aligned}
&\frac{\partial}{\partial\theta}\{(1 + r/R \sin\theta)\mathcal{H}_z\} - i\gamma_c r\mathcal{H}_\theta + i\omega\epsilon r(1 + r/R \sin\theta)\mathcal{E}_e = 0 \\
&i\gamma_c\mathcal{H}_r - \frac{\partial}{\partial r}\{(1 + r/R \sin\theta)\mathcal{H}_z\} + i\omega\epsilon(1 + r/R \sin\theta)\mathcal{E}_\theta = 0 \\
&\frac{\partial}{\partial r}(r\mathcal{H}_\theta) - \frac{\partial}{\partial\theta}\mathcal{H}_r + i\omega\epsilon r\mathcal{E}_z = 0 \\
&\frac{\partial}{\partial\theta}\{(1 + r/R \sin\theta)\mathcal{E}_z\} - i\gamma_c\mathcal{E}_\theta - i\omega\mu r(1 + r/R \sin\theta)\mathcal{H}_r = 0 \\
&i\gamma_c\mathcal{E}_r - \frac{\partial}{\partial r}\{(1 + r/R \sin\theta)\mathcal{E}_z\} - i\omega\mu(1 + r/R \sin\theta)\mathcal{H}_\theta = 0 \\
&\frac{\partial}{\partial r}(r\mathcal{E}_\theta) - \frac{\partial}{\partial\theta}\mathcal{E}_r - i\omega\mu r\mathcal{H}_z = 0
\end{aligned} \tag{31}$$

where we have omitted the common factor

$$\exp i(\gamma_c z - \omega t)$$

in which γ_c is the propagation constant along the curved z-axis.

The toroidal system (r, θ, z) and the curved waveguide degenerate into a cylindrical system and a straight guide, respectively, as R approaches infinity. Maxwell's equations for the straight guide are therefore obtained from (31) by letting $R \to \infty$.

$$\begin{aligned}
\frac{\partial}{\partial\theta} H_z - i\gamma r H_\theta + i\omega\epsilon r E_r &= 0 \\
i\gamma H_r - \frac{\partial}{\partial r} H_z + i\omega\epsilon E_r &= 0 \\
\frac{\partial}{\partial r}(rH_\theta) - \frac{\partial}{\partial\theta} H_r + i\omega\epsilon r E_r &= 0 \\
\frac{\partial}{\partial\theta} E_z - i\gamma r E_\theta - i\omega\epsilon r H_r &= 0 \\
i\gamma E_r - \frac{\partial}{\partial r} E_z - i\omega\mu H_\theta &= 0 \\
\frac{\partial}{\partial r}(rE_\theta) - \frac{\partial}{\partial\theta} E_r - i\omega\mu r H_z &= 0
\end{aligned} \tag{32}$$

where γ is the propagation constant for the straight guide, and the superscript i and subscripts nm are suppressed.

IX. SOLUTION FOR THE CURVED GUIDE

We proceed to solve (31) for the field vectors $\vec{\mathcal{E}}$, $\vec{\mathcal{H}}$ and obtain the propagation constant γ_c for the curved guide as functions of the field vectors $\vec{E}$, $\vec{H}$ and the propagation constant γ of the straight guide. The latter quantities are known [(2), (3), (4) and (20)]. We introduce a parameter

$$\sigma = \frac{k}{\gamma - k} \cdot \frac{a}{R} \approx 2\left(\frac{2\pi a}{u_{nm}\lambda}\right)^2 \frac{a}{R}. \tag{33}$$

The range of interest is that for which the radius of curvature R is so large that $\sigma \ll 1$.

Using a first-order perturbation technique, the solution of (31) is

$$\begin{aligned}
\mathcal{E}_\theta &= (1 + \sigma r/a \sin\theta)E_\theta \\
\mathcal{E}_r &= (1 + \sigma r/a \sin\theta)E_r \\
\mathcal{E}_z &= (1 + \sigma r/a \sin\theta)E_z + (i\sigma/ka)(E_r \sin\theta + E_\theta \cos\theta) \\
\mathcal{H}_\theta &= (1 + \sigma r/a \sin\theta)H_\theta \\
\mathcal{H}_r &= (1 + \sigma r/a \sin\theta)H_r \\
\mathcal{H}_z &= (1 + \sigma r/a \sin\theta)H_z + (i\sigma/ka)(H_r \sin\theta + H_\theta \cos\theta).
\end{aligned} \tag{34}$$

The effect of curvature of the guide axis is to make unsymmetrical the

transverse field configuration of the straight guide. Each transverse component is enhanced in the half cross section farthest from the center of curvature.

To a first-order perturbation of σ, the propagation constants of the curved and straight guide are identical; i.e., $\gamma_c \approx \gamma$. Nevertheless, knowing the field components of the mildly curved structure, it is possible to calculate its attenuation constants $\alpha_{nm}(R) = \text{Re}\ \gamma_c$.

X. ATTENUATION CONSTANTS $\alpha_{nm}(R)$

The mean radial power flowing into the dielectric per unit length at the surface of the guide is

$$P_r = \frac{1}{2}\int_0^{2\pi} \text{Re}\,[\mathcal{E}_\theta \mathcal{H}_z^* - \mathcal{E}_z \mathcal{H}_\theta^*]_{r=a}\,[1 + a/R \sin\theta] a\, d\theta. \tag{35}$$

The power flow in the axial z direction within the internal medium $r < a$ is

$$P_z = \frac{1}{2}\int_0^a \int_0^{2\pi} \text{Re}\,[\mathcal{E}_r \mathcal{H}_\theta^* - \mathcal{E}_\theta \mathcal{H}_r^*] r\, d\theta\, dr \tag{36}$$

and decreases along z at a rate equal to the radial flow per unit length P_r; i.e.,

$$\frac{dP_z}{dz} = -2\alpha_{nm}(R) P_z = -P_r \tag{37}$$

where $\alpha_{nm}(R)$ is the attenuation constant of the mode under consideration for the curved hollow dielectric waveguide. Consequently

$$\alpha_{nm}(R) = \tfrac{1}{2}(P_r/P_z). \tag{38}$$

To compute P_r we substitute the known field quantities into (35). This yields

$$P_r = \text{Re}\sqrt{\frac{\epsilon_0}{\mu_0}}\frac{u_{nm}^2 J_n^2(u_{nm})}{2k^2 a\sqrt{\nu^2 - 1}}\int_0^{2\pi} |1 + \sigma \sin\theta|^2 (1 + a/R \sin\theta) \begin{cases} 1 & \text{for } TE_{0m} \text{ modes} \\ \nu^2 & \text{for } TM_{0m} \text{ modes} \\ \nu^2 \sin^2 n(\theta + \theta_0) + \cos^2 n(\theta + \theta_0) & \text{for } EH_{nm} \text{ modes.} \end{cases} d\theta \tag{39}$$

Terms with powers of $\lambda/(2\pi a)$ larger than two have been neglected. Upon integrating,

$$P_r = \pi\ \text{Re}\sqrt{\frac{\epsilon_0}{\mu_0}}\frac{u_{nm}^2 J_n^2(u_{nm})}{k^2 a\sqrt{\nu^2 - 1}}$$

$$\begin{cases} (1 + \frac{1}{2}\sigma^2) & \text{for } TE_{0m} \text{ modes} \\ \nu^2(1 + \frac{1}{2}\sigma^2) & \text{for } TM_{0m} \text{ modes} \\ \frac{1}{2}(\nu^2 + 1)\left[1 + \frac{1}{2}\sigma^2\left(1 + \frac{\delta_n(\pm 1)}{2}\frac{\nu^2 - 1}{\nu^2 + 1}\cdot\cos 2\theta_0\right)\right] & \text{for } EH_{nm} \text{ modes} \end{cases} \tag{40}$$

where

$$\delta_n(\pm 1) = \begin{cases} 1, & n = \pm 1 \\ 0, & n \neq \pm 1. \end{cases} \tag{41}$$

The power P_z flowing radially in the guide is obtained by substituting (34) into (36) and integrating

$$P_z = \frac{\pi a^2}{2}\sqrt{\frac{\epsilon_0}{\mu_0}}\, J_n^2(u_{nm})\left\{1 + \frac{\sigma^2}{6}[1 + 2n(n-2)/u_{nm}^2]\right\}. \tag{42}$$

Hence

$$\alpha_{nm}(R) = \alpha_{nm}(\infty)\left\{1 + \frac{4}{3}\left(\frac{2\pi a}{u_{nm}\lambda}\right)^4\left(\frac{a}{R}\right)^2 \cdot\left[1 - \frac{n(n-2)}{u_{nm}^2} + \frac{3}{4}\delta_n(\pm 1)\frac{\operatorname{Re}\sqrt{\nu^2 - 1}}{\operatorname{Re}\dfrac{\nu^2 + 1}{\sqrt{\nu^2 - 1}}}\cos 2\theta_0\right]\right\} \tag{43}$$

where $\alpha_{nm}(\infty) = \alpha_{nm}$ is the attenuation constant for modes in the straight guide ($R = \infty$) given by (21). The attenuation constant $\alpha_{nm}(R)$ can also be written in the following form

$$\alpha_{nm}(R) = \alpha_{nm}(\infty) + (a^3/\lambda^2 R^2)\operatorname{Re} V_{nm}(\nu) \tag{44}$$

where

$$V_{nm}(\nu) = \frac{4}{3}\begin{Bmatrix} \dfrac{1}{\sqrt{\nu^2 - 1}} \\ \dfrac{\nu^2}{\sqrt{\nu^2 - 1}} \\ \dfrac{\frac{1}{2}(\nu^2 + 1)}{\sqrt{\nu^2 - 1}} \end{Bmatrix}\left(\frac{2\pi}{u_{mn}}\right)^2 \cdot\left\{1 - \frac{n(n-2)}{u_{nm}^2} + \frac{3}{4}\delta_n(\pm 1)\left(\frac{\nu^2 - 1}{\nu^2 + 1}\right)\cos 2\theta_0\right\}. \tag{45}$$

The values of $\mathrm{Re}V_{nm}(\nu)$ are always positive. Some of them have been calculated in Table II for a refractive index $\nu = 1.50$.

The attenuation constant of any mode consists of two terms (44). The first coincides with that of the straight guide and is proportional to $u_{nm}{}^2\lambda^2/a^3$; the second term represents an increase in attenuation due to curvature of the guide axis and is proportional to $a^3/\lambda^2R^2u_{nm}{}^2$. Therefore the lower the straight guide attenuation constant (small $u_{nm}{}^2\lambda^2/a^3$), the larger the loss due to bends and vice versa. From (43) or (45) we find that only for the $EH_{\pm 1,m}$ modes, the orientation of the field with respect to the plane of curvature influences the attenuation. If $\theta_0 = 0$, the electric field in the center of the guide is in the plane of curvature and the attenuation is a maximum. For $\theta_0 = \pm\pi/2$, the electric field is normal to the plane of curvature and the attenuation is a minimum. The ratio of maximum to minimum is mild, however. For the lowest attenuation mode EH_{11} and $\nu = 1.50$, it is

$$\frac{V_{nm}(\theta_0 = 0)}{V_{nm}(\theta_0 = \pi/2)} = 1.65. \tag{46}$$

If $|\nu| \gg 1$, that ratio is

$$\frac{V_{nm}(\theta_0 = 0)}{V_{nm}(\theta = \pi/2)} = 4.6.$$

From equation (43) we find that the radius of curvature which doubles the straight guide attenuation is

$$R_0 = \frac{2}{\sqrt{3}}\left(\frac{2\pi}{u_{mn}}\right)^2\frac{a^3}{\lambda^2} \cdot\left[1 - \frac{n(n-2)}{u_{nm}{}^2} + \frac{3}{4}\delta_n(\pm 1)\,\mathrm{Re}\,\frac{\mathrm{Re}\,\sqrt{\nu^2-1}}{\nu^2+1}\cos 2\theta_0\right]^{\frac{1}{2}}. \tag{47}$$

This value of R_0 is only approximate since (43) was derived by assuming $\sigma \ll 1$.

XI. EFFECT OF CURVATURE ON ATTENUATION OF MODES IN THE HOLLOW DIELECTRIC WAVEGUIDE

For a straight hollow glass waveguide with $\nu = 1.5$ and a radius $a = 1$ mm operating typically at a wavelength $\lambda = 1\mu$, the attenuation of the lowest-loss mode EH_{11} is $\alpha_{11} = 1.85$ db/km. This loss is doubled for a radius of curvature $R_0 \approx 10$ km. For long distance optical transmission a radius of curvature of at least a few hundred meters would

TABLE II — SOME VALUES OF $V_{nm}(\nu)$

n/m		1	2	3	4
-1		$2.57\ (1 + 0.326 \cos 2\theta_0)$	$1.034\ (1 + 0.301 \cos 2\theta_0)$	$0.553\ (1 + 0.295 \cos 2\theta_0)$	$0.347\ (1 + 0.293 \cos 2\theta_0)$
0	TE	3.22	0.955	0.455	0.265
	TM	7.22	2.145	1.022	0.596
1		$15.5\ (1 + 0.246 \cos 2\theta_0)$	$2.60\ (1 + 0.279 \cos 2\theta_0)$	$1.034\ (1 + 0.284 \cos 2\theta_0)$	$0.554\ (1 + 0.286 \cos 2\theta_0)$
2		5.22	1.55	0.735	0.432
3		2.57	1.034	0.553	0.347
4 or -2		1.51	0.737	0.430	0.287

be tolerable. Therefore hollow dielectric waveguides do not seem suitable for long distance optical transmission.

On the other hand, the curvature in hollow dielectric waveguides for application in gaseous amplifiers and oscillators is not critical. For example, if $a = 0.25$ mm and $\lambda = 1\mu$, the straight guide attenuation is 0.12 db/meter. The radius of curvature which doubles this quantity for the lossiest polarization — i.e., with the electric field at the center of the guide contained in the plane of curvature — is approximately 150 meters, a value well within the limits of laboratory precision. Consequently, the hollow dielectric waveguide does remain very attractive as a guiding medium for optical amplifiers and oscillators where a small guide radius is desirable, thereby making the guide less sensitive to curvature of the axis.

XII. EFFECT OF CURVATURE ON ATTENUATION OF MODES IN THE METALLIC GUIDE

The attenuation constants $\alpha_{0m}(R)$ for the lowest-loss TE_{0m} modes in the curved metallic guide are given by

$$\alpha_{0m}(R) \approx \alpha_{0m}(\infty) \left\{1 + \frac{4}{3}\left(\frac{2\pi a}{\lambda u_{0m}}\right)^4 \left(\frac{a}{R}\right)^2\right\} \tag{48}$$

where $\alpha_{0m}(\infty)$ is the attenuation constant for the TE_{0m} mode in the straight guide, $R = \infty$. For a radius $a = 0.25$ mm and wavelength $\lambda = 1\mu$, the straight guide loss for the lowest-loss TE_{01} mode, $\alpha_{01}(\infty) = 1.8$ db/km, is doubled for a radius of curvature of only $R_0 \approx 48$ meters.

For $\lambda = 3\mu$ and $a = 0.6$ mm, the straight TE_{01} loss is also 1.8 db/km and the radius of curvature that doubles that loss is 75 m.

XIII. CONCLUSIONS

The hollow dielectric waveguide at optical wavelengths supports a complete set of normal modes that are either circular electric, circular magnetic or hybrid. They resemble the modes found in a sequence of circular irises not only in field configuration but also in loss discrimination among them. For hollow metallic waveguides the mode discrimination is far larger.

The field configuration and propagation constants have been determined. The attenuation is practically independent of the loss tangent of the dielectric but depends essentially on the refraction mechanism at the wall. Assuming refractive index of the dielectric, 1.5 for hollow dielectric waveguides, the EH_{11} mode exhibits the lowest power attenuation, viz., 1.85 (λ^2/a^3) db/m. For a wavelength $\lambda = 1\mu$ and a tube radius $a = 1$ mm, the attenuation is only 1.85 db/km.

The hollow dielectric waveguide does not, however, seem suitable for long distance optical transmission because of the high loss introduced by even mild curvature of the guide axis. Nevertheless it remains very attractive as a guiding medium for optical amplifiers and oscillators, since here a small radius of the guide is desirable. Consequently, curvature of the guide axis is not critical. Filled with "masing" material, the hollow dielectric waveguide provides not only guidance but also gain which is almost inversely proportional to the radius. For the right He-Ne mixture, the maximum theoretical gain attainable is 7.6 db/m provided that the radius is 0.058 mm. But even if the radius is 0.25 mm, the predicted gain is still large, viz. 2.6 db/m.

The metallic waveguide is superior to the hollow dielectric waveguide for use in long distance optical transmission. Because of the relatively large dielectric constant exhibited by aluminum at optical frequencies, the attenuation constant for the lowest-loss mode TE_{01} is comparatively small and less sensitive to curvature of the guide axis. For a radius $a = 0.25$ mm and a wavelength $\lambda = 1\mu$, the attenuation constant for TE_{01} modes in the straight aluminum guide is only 1.8 db/km, which is doubled for a radius of curvature of about 48 meters. For $a = 0.6$ mm and $\lambda = 3\mu$, the TE_{01} straight guide loss is also 1.8 db/km but is doubled if the radius of curvature of the waveguide axis is 75m.

We have considered some of the theoretical problems of the hollow dielectric or metallic waveguide. The results are promising. Nevertheless, the usefulness of these guides has yet to be proven experimentally,

and furthermore the attenuation constants discussed here do not include scattering losses due to surface imperfections.

XIV. ACKNOWLEDGMENTS

It is a pleasure to thank R. Kompfner and S. E. Miller for their suggestions.

REFERENCES

1. Fox, A. G., and Li, Tingye, Resonant Modes in a Maser Interferometer, B.S.T.J., **40**, March, 1961, p. 453.
2. Boyd, G. D., and Gordon, J. P., Confocal Multimode Resonator for Millimeter through Optical Wavelength Masers, B.S.T.J., **40**, March, 1961, p. 489.
3. Boyd, G. D., and Kogelnik, H., Generalized Confocal Resonator Theory, B.S.T.J., **41**, July, 1962, p. 1347.
4. Goubau, G., and Schwering, F., On the Guided Propagation of Electromagnetic Wave Beams, Trans. I.R.E., **AP-9**, May 1961, p. 248.
5. Eaglesfield, C. C., Optical Pipeline: A Tentative Assessment, The Inst. of Elect. Engineers, January, 1962, p. 26.
6. Simon, J. C., and Spitz, E., Propagation Guidée de Lumière Cohérente, J. Phys. Radium, **24**, February, 1963, p. 147.
7. Goubau, G., and Christian, J. R., Some Aspects of Beam Waveguides for Long Distance Transmission at Optical Frequencies, IEEE Trans. on Microwave Theory and Techniques, **MTT-12**, March, 1964, pp. B.S.T.J., 212–220.
8. Marcuse, D., and Miller, S. E., Analysis of a Tubular Gas Lens, B.S.T.J., this issue, p. 1759.
9. Berreman, D. W., A Lens or Light Guide Using Convectively Distorted Thermal Gradients in Gases, B.S.T.J., this issue, p. 1469.
10. Berreman, D. W., A Gas Lens using Unlike, Counter-Flowing Gases, B.S.T.J., this issue, p. 1476.
11. Gordon, E. I., and White, A. D., Similarity Laws for the He-Ne Gas Maser, Appl. Phys. Letters, **3**, December 1, 1963, p. 199.
12. Stratton, J. A., *Electromagnetic Theory*, McGraw-Hill Book Co., New York and London, 1941, p. 524.
13. Hodgson, J. N., Proc. Phys. Soc. (London), **B68**, 1955, p. 593.
14. Beattie, J. R., and Conn, G. K. T., Phil. Mag., **7**, 1955, pp. 46, 222, and 989.
15. Schulz, L. G., J. Opt. Soc. Am., **41**, 1951, p. 1047; **44**, 1954 p. 357.
16. Givens, M. Parker, Optical Properties of Metals, *Solid State Physics*, **6**, Acad. Press Inc., New York, 1958, p. 313.